Supporting Information for: Precipitating Polyelectrolyte-Surfactant Systems by Admixing a Nonionic Surfactant – a Case of Cononsurfactancy

Leonardo Chiappisi,[*,†,‡] Stephen David Leach,[†] and Michael Gradzielski[*,†]

Stranski Laboratorium für Physikalische Chemie und Theoretische Chemie, Institut für Chemie, Strasse des 17. Juni 124, Sekr. TC7, Technische Universität Berlin, D-10623 Berlin, Germany, and Institut Max von Laue - Paul Langevin, Large Scale Structures Group, 71 avenue des Martyrs - 38042 Grenoble Cedex 9

E-mail: leonardo.chiappisi@tu-berlin.de; michael.gradzielski@tu-berlin.de

Contents

*To whom correspondence should be addressed
†Technische Universität Berlin
‡Institut Laue - Langevin

1 Experimental details

Table S1: Densities, scattering length densities (SLD), and volumes (v used in for the description of the SANS experimental results. SLDs and densities are obtained considering solvent-exchangeable protons.

Compound	Density / g cm^{-3}	SLD / 10^{-4} nm^{-2}	v / nm^3
Acetic acid buffer	1.10	6.27	—
Chitosan	1.17	2.86	0.223
$C_{18:1}$	0.85	-0.36	0.494
$(OCH_2CH_2)_9OCH_2COOH$	1.23	0.99	0.600
$(OCH_2CH_2)_9OH$	1.19	0.82	0.576

Light scattering Static (SLS) and dynamic (DLS) light scattering measurements were performed simultaneously on the mixed micelle solutions on the same compact ALV/CGS-3 instrument, equipped with a He-Ne laser with a wavelength of $\lambda = 632.8$ nm. The results are reported in section 2.6 of the supporting information. Experiments were performed at scattering angles θ ranging from 20° to 130° set with an ALV-SP 125 goniometer. Pseudo-cross correlation functions were recorded using an ALV 5000/E multiple-τ correlator. All measurements were carried out at 25.0(1) °C in a thermostatted toluene bath.

Absolute scattering intensities were obtained using toluene as a standard, where a Rayleigh ratio of 1.340×10^{-5} cm^{-1} for 25 °C and 632.8 nm was used.[1] Isotropic scattering is observed from the mixed micelle solutions investigated, and the forward scattering intensity $I(0)$ is obtained from the average of the intensities recorded between 20° to 130°. The apparent molecular weight of the micelles of a solution of concentration c, is obtained by means of the following relation:

$$M_w^{app} = \frac{I(0)}{K_L c} \tag{S1}$$

with K_L being the optical constant:

$$K_L = \frac{4\pi^2}{\lambda^4 N_A} n_0^2 \left(\frac{\mathrm{d}n}{\mathrm{d}c}\right)^2 \tag{S2}$$

where N_A is the Avogadro constant, n_0 is the refractive index of the solvent and $\mathrm{d}n/\mathrm{d}c \approx 0.119$ cm^3 g^{-1} is the refractive index increment. Due the high concentration of acetic acid/sodium acetate in the buffer, there is no need to take into account the scattering structure factor for the surfactant micelle solution.[2] The micelle aggregation numbers were obtained neglecting the free surfactant concentration, as justified by the very low cmc of $\sim 6 \cdot 10^{-6} molL^{-1}$ for $C_{18:1}E_9CH_2COOH$.

The mean decay rate $\overline{\Gamma}(q)$ was obtained from the field autocorrelation function:[3]

$$g^{(1)}(\tau, q) = \exp\left(-\overline{\Gamma}(q)\tau\right)\left(1 + \frac{\mu_2}{2}\tau^2\right) \tag{S3}$$

where τ and μ_2 are the delay time and the second moment around the mean, respectively. The apparent diffusion coefficient is obtained as $D_{app} = \overline{\Gamma}(q)/q^2$, from which the hydrodynamic radius (R_h) was obtained, applying the Stokes-Einstein relation:

$$R_h = \frac{k_b T}{6\pi\eta_0 D_{app}} \tag{S4}$$

with η_0 being the solvent viscosity.

Zeta-potential determination The electrophoretic mobility μ_e of the mixed micelles was determined on a Malvern Zetasizer Nano Z, equipped with a He-Ne laser (633 nm). The ζ-potential of the mixed micelles was calculated as:

$$\zeta = \frac{3\mu_e \eta}{2\varepsilon_0 \varepsilon_r f(\kappa a)} \tag{S5}$$

with η being the fluid viscosity, ε_0 the vacuum permittivity, ε_r the relative permittivity, and $f(\kappa a)$ is the Henry function approximated by:[4]

$$f(\kappa a) = \frac{16 + 18\kappa a + 3(\kappa a)^2}{16 + 18\kappa a + 2(\kappa a)^2} \tag{S6}$$

where κ is the inverse Debye length while a is the particle size approximated by its hydrodynamic radius.

^{1}H-NMR of surfactants The ^{1}H-NMR spectrum of $C_{18:1}E_9CH_2COOH$ and $C_{18:1}E_9$ solubilized in $CDCl_3$ was recorded on a Brucker Avance II spectrometer operating at 400 MHz. The spectra are reported in Figs. S1 and S2. From the integral of the different peaks, we deduced that the alkyl chain is a 3:1 mixture of oleyl and palmitic alcohol, while on average 8.8 EO units per surfactant chains are present. The degree of carboxymethylation is of ~ 0.9, in agreement with previous results from pH titrations.[2] In Table S2 the predicted and experimentally determined integrals of the ^{1}H-NMR peaks. In each spectrum one unidentified peak is present: for $C_{18:1}E_9CH_2COOH$ a very broad peak is observed at $\delta = 5.6$ ppm, representing 3.5 % of the hydrogens in the sample; for $C_{18:1}E_9$ a singlet at 3.3 ppm, representing 2 % of the hydrogens in the sample, is present.

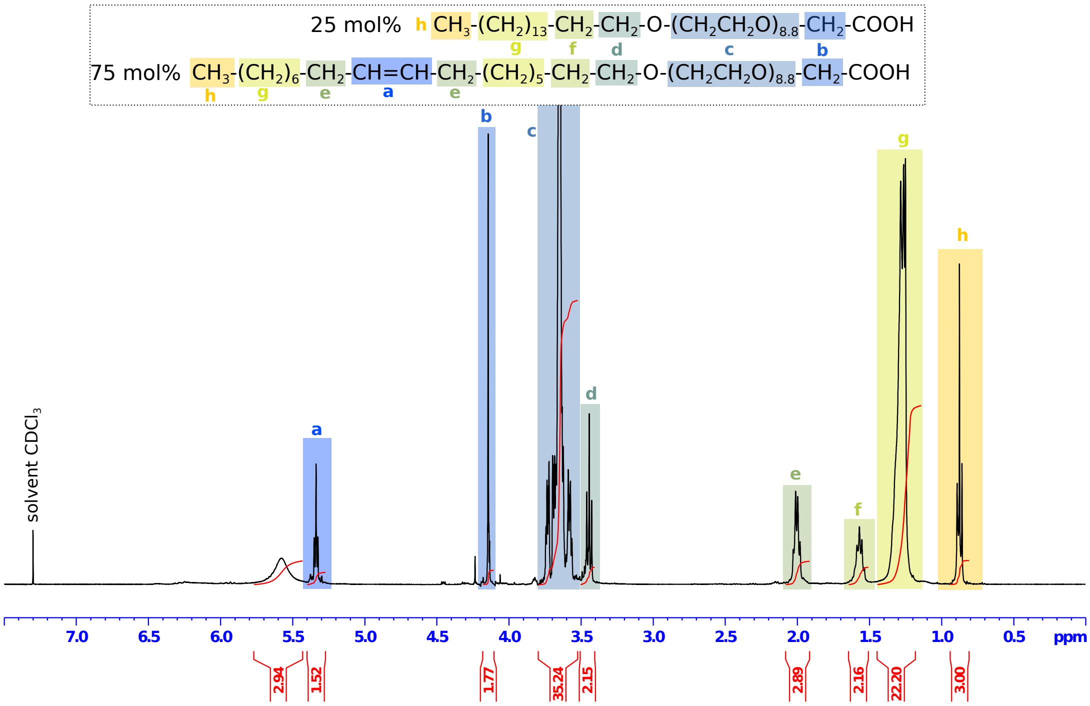

Figure S1: [1]H-NMR spectrum (400 MHz, $CDCl_3$) of $C_{18:1}E_9CH_2COOH$.

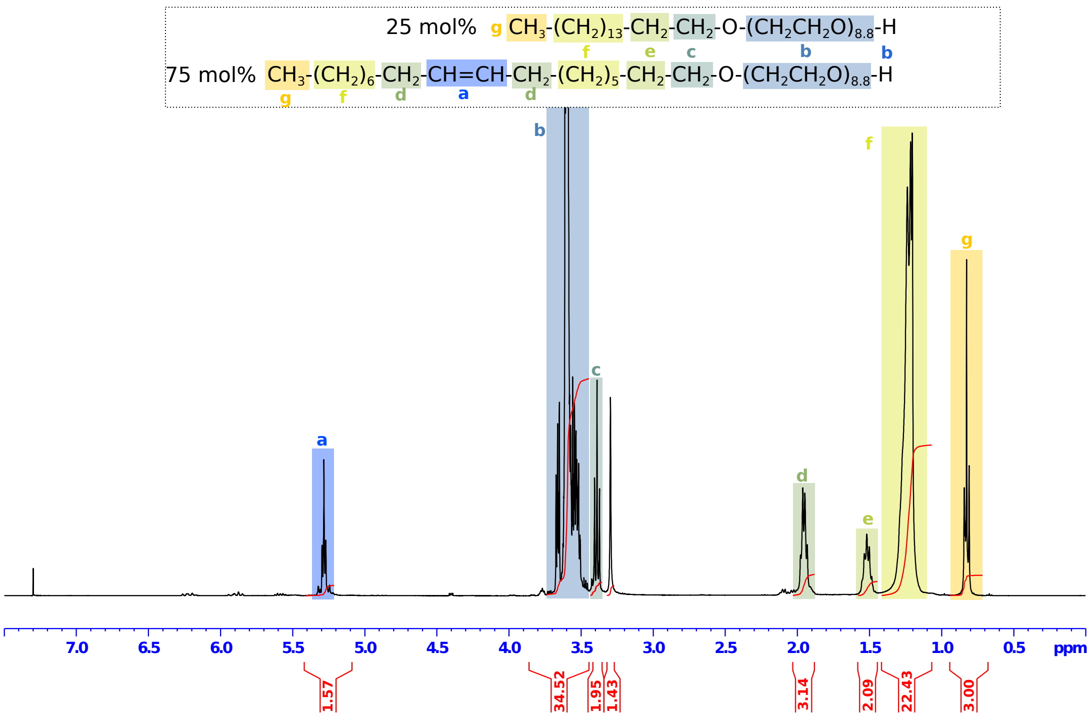

Figure S2: [1]H-NMR spectrum (400 MHz, $CDCl_3$) of $C_{18:1}E_9$.

Table S2: Characterization of ^{1}H-NMR spectra from $C_{18:1}E_9CH_2COOH$ (left) and $C_{18:1}E_9$ (right). Chemical shift δ is given in ppm, in parentheses the letter used for their identification in Figs. S1 and S2 is provided. Experimentally I^{exp} and calculated I^{cal} integrals are normalized with respect to the three hydrogen of the terminal CH_3 group.

δ	I^{exp}	I^{cal}
0.9 (h)	3.0	3
1.2 (g)	22.2	23
1.5 (f)	2.2	2
2.0 (e)	2.9	3
3.4 (d)	2.1	2
~3.6 (c)	35.2	35.2
4.2 (b)	1.8	1.8
5.3 (a)	1.5	1.5

δ	I^{exp}	I^{cal}
0.9 (g)	3.0	3
1.2 (f)	22.4	23
1.5 (e)	2.1	2
2.0 (d)	3.1	3
3.4 (c)	2.0	2
~3.6 (b)	34.5	35.2
5.3 (a)	1.6	1.5

2 Additional results

2.1 Pictures of Samples

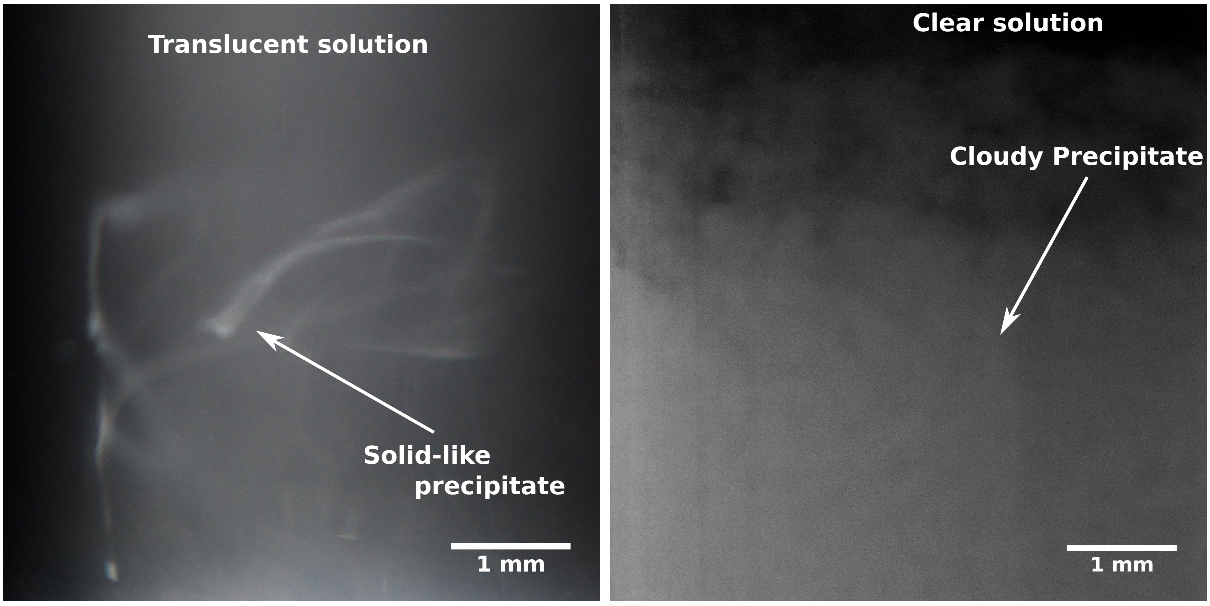

Figure S3: Picture of two samples in within the two-phase region, with a total chitosan content of 0.3 wt%, Z = 0.2, χ = 0.4, and pH 5.0 on the left and ca. 10 on the right. Picture evidence a homogenous, cloudy precipitate with a clear surnatant at high pH, while the formation of a solid-like precipitate in equilibrium with a translucent solution. The sample on the left, at pH 5 was gently shaken before taking the picture in order to disperse the precipitate.

2.2 Additional phase diagrams

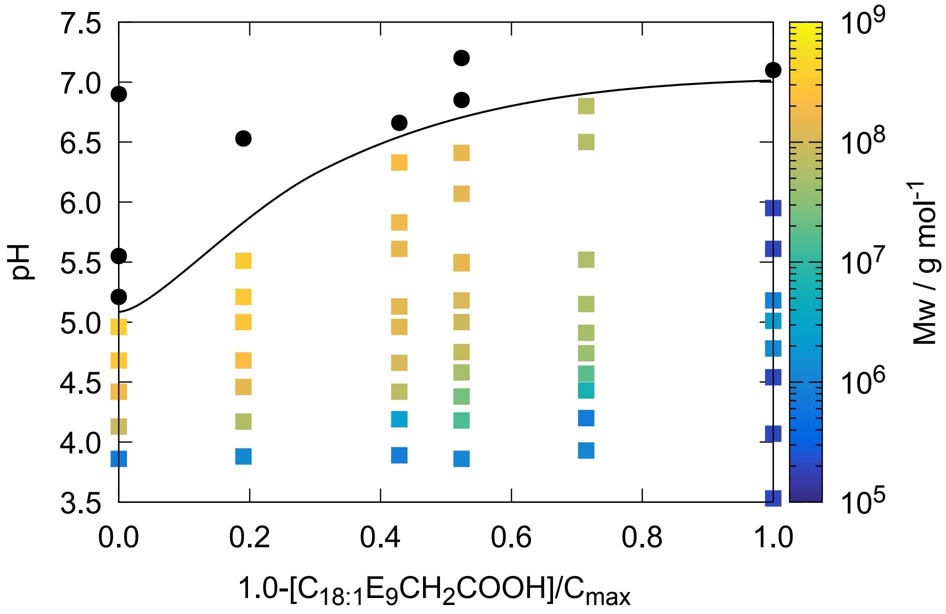

Figure S4: Phase behavior of chitosan - $C_{18:1}E_9CH_2COOH$ mixtures, with a chitosan content of 0.3 wt% as a function of pH and $C_{18:1}E_9CH_2COOH$ concentration. The atypical x-axis, with $C_{max} = 3.6\ 10^{-3}$ mol kg^{-1}, corresponding to a mixing ratio $Z = 0.2$ was chosen in order to have a direct relation with Fig. 2 of the main text, with $x = 0.0$ representing mixtures chitosan - $C_{18:1}E_9CH_2COOH$ while $x = 1.0$ represents pure chitosan solutions. The M_w obtained *via* turbidimetry are expressed with the colour gradient reported on the right. Full black circles represent samples showing phase separation, squares with variable colour represent monophasic samples.

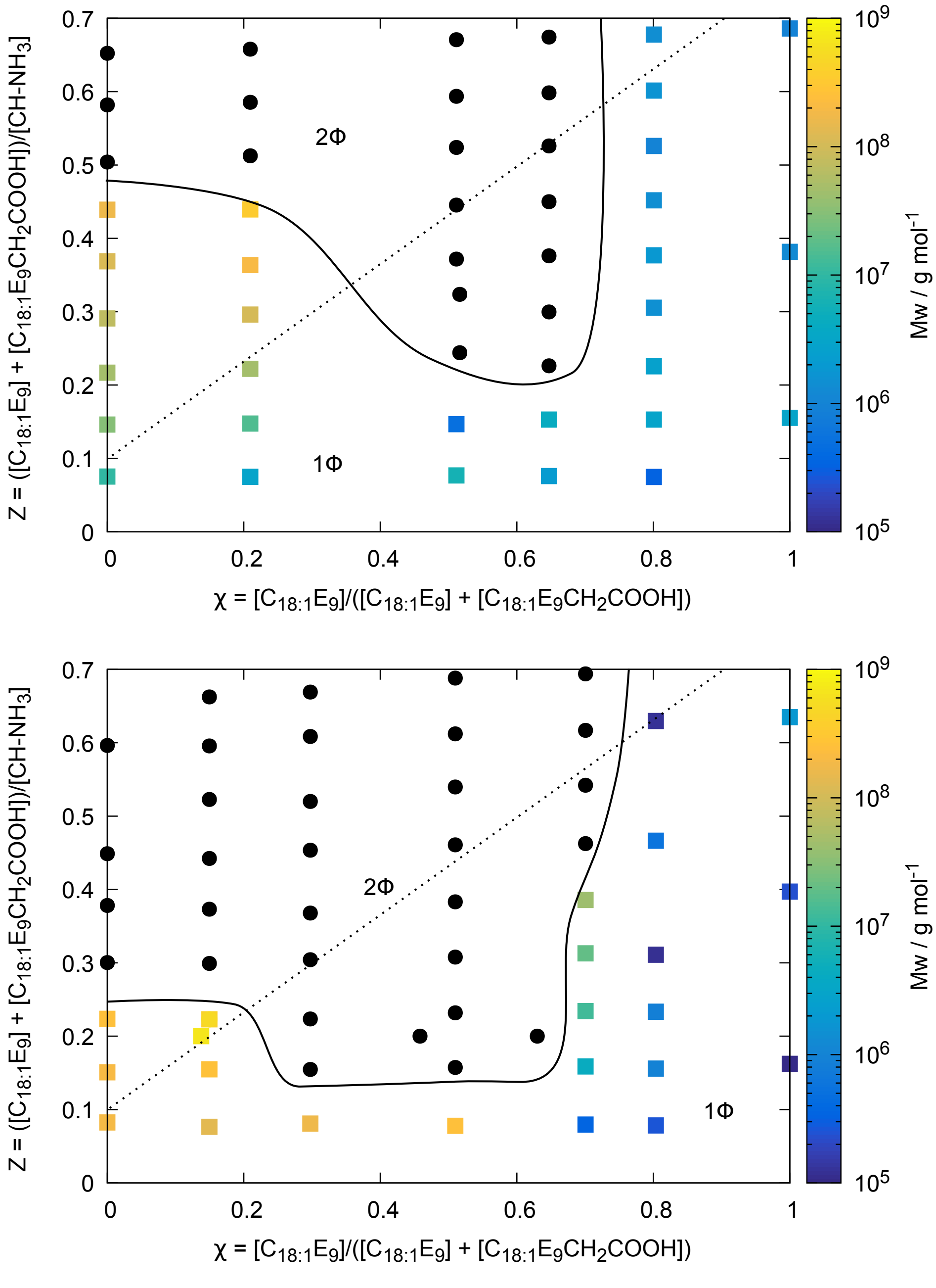

Figure S5: Phase behavior of chitosan - $C_{18:1}E_9CH_2COOH$ and $C_{18:1}E_9$ mixtures, with a chitosan content of 0.3 wt%, pH = 4.0 on the top and 4.75 on the bottom, as a function of Z and χ. The M_w obtained *via* turbidimetry are expressed with the colour gradient reported on the right. Full black circles represent samples showing phase separation, squares with variable colour represent monophasic samples. Dashed lines represent composition values with constant $C_{18:1}E_9CH_2COOH$ content, i.e. constant charge ratio.

2.3 Molecular weight of complexes

In table S3 the molecular weight of the complexes reported in Fig. 1 of the main text are reported. The molecular weights were obtained *via* turbidimetric measurements, as described in the experimental section of the main text.

Table S3: Molecular weights determined by turbidity measurements for the aggregates of chitosan (0.3 wt%), at variable pH and χ as reported in Fig. 1 of the main text.

χ	pH	Mw / g mol^{-1}	χ	pH	Mw / g mol^{-1}	χ	pH	Mw / g mol^{-1}
0.00	3.5	$6.4\cdot10^5$	0.45	3.8	$3.7\cdot10^5$	0.80	5.5	$1.4\cdot10^6$
0.00	3.7	$5.5\cdot10^5$	0.45	4.1	$5.4\cdot10^6$	0.80	6.0	$1.6\cdot10^6$
0.00	3.9	$1.1\cdot10^7$	0.45	4.2	$3.8\cdot10^7$	0.80	6.2	$1.4\cdot10^6$
0.00	4.0	$2.3\cdot10^7$	0.45	4.3	$8.9\cdot10^7$	0.80	6.6	$1.4\cdot10^6$
0.00	4.1	$3.5\cdot10^7$	0.45	6.3	$7.3\cdot10^7$	0.80	6.9	$6.7\cdot10^7$
0.00	4.3	$5.4\cdot10^7$	0.45	6.5	$1.1\cdot10^7$			
0.00	4.4	$7.1\cdot10^7$	0.45	6.8	$7.7\cdot10^6$	0.91	3.4	$8.5\cdot10^4$
0.00	4.6	$9.3\cdot10^7$				0.91	3.7	$6.0\cdot10^4$
0.00	4.8	$1.1\cdot10^8$				0.91	4.0	$2.5\cdot10^5$
0.00	5.1	$1.3\cdot10^8$	0.64	3.6	$1.9\cdot10^6$	0.91	4.2	$1.3\cdot10^6$
			0.64	3.9	$3.1\cdot10^6$	0.91	4.3	$1.7\cdot10^6$
			0.64	4.0	$6.4\cdot10^6$	0.91	4.6	$1.6\cdot10^6$
0.14	3.7	$4.9\cdot10^4$	0.64	6.3	$8.0\cdot10^6$	0.91	4.7	$1.7\cdot10^6$
0.14	4.0	$2.1\cdot10^7$	0.64	6.8	$2.8\cdot10^6$	0.91	5.0	$1.7\cdot10^6$
0.14	4.1	$7.9\cdot10^7$				0.91	5.5	$2.8\cdot10^6$
0.14	4.2	$1.3\cdot10^8$				0.91	5.9	$3.0\cdot10^6$
0.14	4.3	$1.8\cdot10^8$	0.72	3.7	$2.4\cdot10^6$	0.91	6.2	$4.0\cdot10^6$
0.14	4.5	$2.5\cdot10^8$	0.72	4.0	$1.2\cdot10^6$	0.91	6.3	$2.4\cdot10^6$
0.14	4.6	$3.3\cdot10^8$	0.72	4.2	$1.2\cdot10^7$	0.91	6.5	$2.8\cdot10^6$
0.14	4.7	$3.7\cdot10^8$	0.72	5.9	$1.2\cdot10^6$	0.91	6.8	$4.8\cdot10^6$
0.14	4.9	$4.1\cdot10^8$	0.72	6.2	$5.6\cdot10^5$			
0.14	5.1	$4.4\cdot10^8$	0.72	6.3	$6.3\cdot10^5$	1.00	3.5	$2.2\cdot10^6$
0.14	5.2	$4.7\cdot10^8$	0.72	6.5	$5.8\cdot10^5$	1.00	3.7	$2.3\cdot10^6$
			0.72	6.7	$4.7\cdot10^6$	1.00	4.0	$2.1\cdot10^6$
						1.00	4.1	$2.2\cdot10^6$
0.33	3.9	$1.1\cdot10^6$	0.80	3.4	$7.4\cdot10^5$	1.00	4.3	$2.1\cdot10^6$
0.33	4.3	$4.4\cdot10^7$	0.80	3.6	$1.1\cdot10^6$	1.00	4.5	$2.3\cdot10^6$
0.33	4.5	$1.3\cdot10^8$	0.80	3.8	$1.4\cdot10^6$	1.00	4.8	$2.3\cdot10^6$
0.32	3.6	$9.4\cdot10^5$	0.80	4.0	$1.5\cdot10^6$	1.00	5.3	$2.3\cdot10^6$
0.32	3.8	$1.8\cdot10^6$	0.80	4.2	$2.6\cdot10^6$	1.00	6.6	$2.5\cdot10^6$
0.32	4.0	$8.0\cdot10^6$	0.80	4.3	$2.7\cdot10^6$			
0.32	4.2	$6.7\cdot10^7$	0.80	4.6	$2.0\cdot10^6$			
0.32	4.2	$1.3\cdot10^8$	0.80	4.9	$1.8\cdot10^6$			
0.32	4.4	$1.9\cdot10^8$	0.80	5.1	$1.4\cdot10^6$			

2.4 Additional ITC titrations

In Fig. S6 the excess mixing heats and according fits for experiments performed at pH 3.75, 4.00, 4.25, 4.50, 4.75, and 5.00 are reported. The obtained parameters are given in Table S4. Fits were performed using Eqs. 4 and 5 reported in the main text.

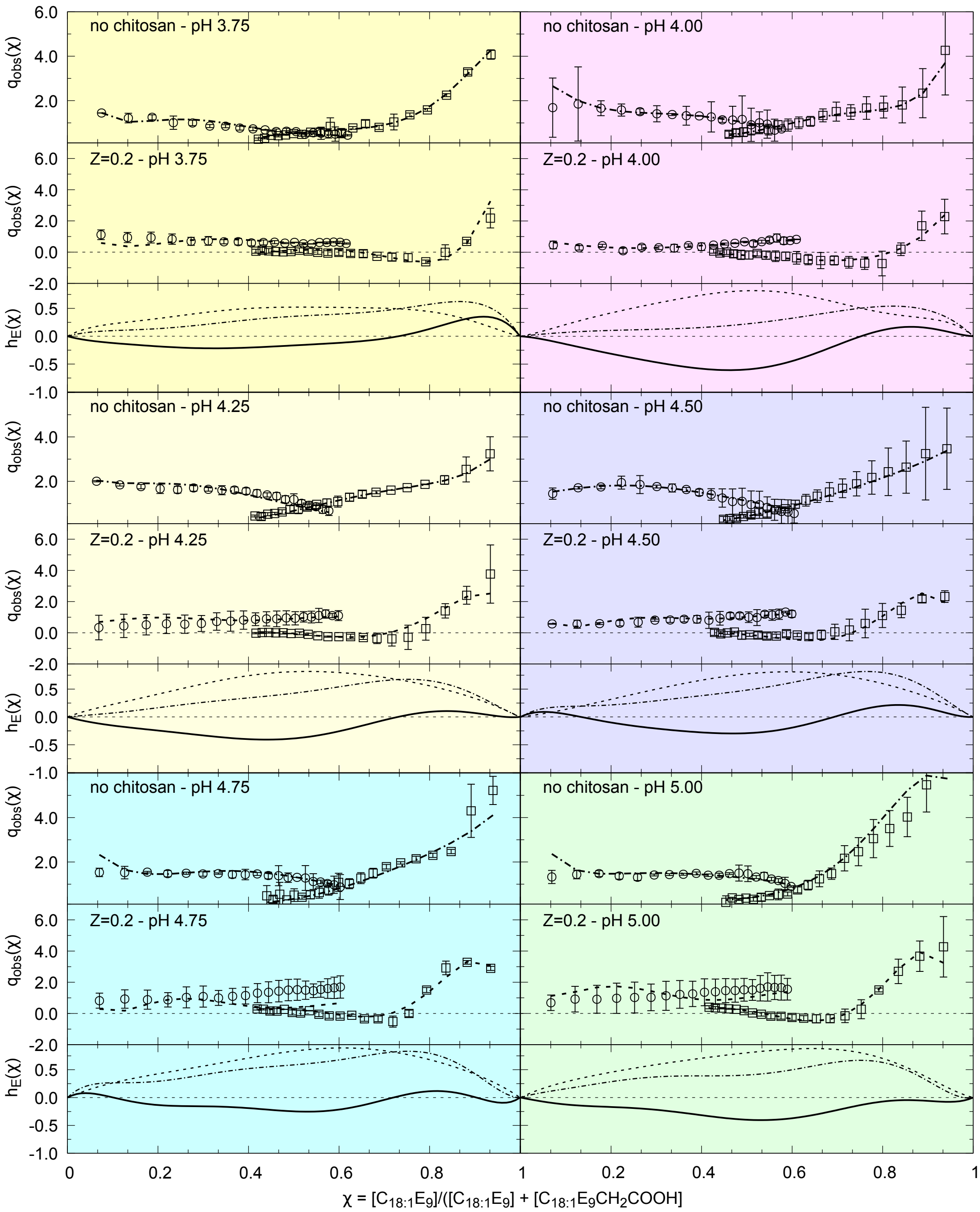

Figure S6: ITC results obtained for titrations performed between pH 3.75 to pH 5.0. q_{obs} are the integrated heats given in kJ mol^{-1}; empty circles are titrations of $C_{18:1}E_9$ into $C_{18:1}E_9CH_2COOH$ (q_1), empty squares are titrations of $C_{18:1}E_9CH_2COOH$ into $C_{18:1}E_9$ (q_2). Dotted and broken lines are best fits with a common set of parameters for q_1 and q_2 *via* Eqs. 4 and 5 in the main text. The excess mixing enthalpies are also reported in kJ mol^{-1} from titration without ($h_E^{Z=\infty}(\chi)$, dotted line) and with chitosan ($h_E^{Z=0.2}(\chi)$, broken line); the excess chitosan-surfactant interaction ($H_E(\chi)$) is represented as thick full line.

Table S4: Fit parameters obtained from ITC. For each investigated pH, the coefficients of the polynomial used in Eq. 2 of the main text with the uncertainties arising from the fitting procedure is reported. The coefficients used for calculating the excess chitosan-surfactant interaction ($H_E(\chi)$) are obtained as the difference between the coefficients for the excess mixing enthalpy obtained in the presence of chitosan $h_E^{Z=0.2}(\chi)$ and without chitosan $h_E^{Z=\infty}(\chi)$.

		pH = 3.75			pH = 4.0			pH = 4.25	
$h_E^{Z=\infty}(\chi)$	ρ_0	$4.35\cdot10^{3}$	$8\cdot10^{2}$	ρ_0	$3.91\cdot10^{3}$	$6\cdot10^{2}$	ρ_0	$2.60\cdot10^{3}$	$1\cdot10^{2}$
	ρ_1	$-3.10\cdot10^{4}$	$9\cdot10^{3}$	ρ_1	$-6.16\cdot10^{3}$	$7\cdot10^{3}$	ρ_1	$-4.71\cdot10^{3}$	$1\cdot10^{3}$
	ρ_2	$1.48\cdot10^{5}$	$4\cdot10^{4}$	ρ_2	$-3.53\cdot10^{3}$	$3\cdot10^{4}$	ρ_2	$3.10\cdot10^{4}$	$4\cdot10^{3}$
	ρ_3	$-3.23\cdot10^{5}$	$8\cdot10^{4}$	ρ_3	$7.47\cdot10^{4}$	$6\cdot10^{4}$	ρ_3	$-5.28\cdot10^{4}$	$6\cdot10^{3}$
	ρ_4	$3.29\cdot10^{5}$	$8\cdot10^{4}$	ρ_4	$-1.36\cdot10^{5}$	$7\cdot10^{4}$	ρ_4	$2.85\cdot10^{4}$	$3\cdot10^{3}$
	ρ_5	$-1.25\cdot10^{5}$	$3\cdot10^{4}$	ρ_5	$7.49\cdot10^{4}$	$3\cdot10^{4}$	ρ_5	—	—
	ρ_6	$-3.97\cdot10^{2}$	$6\cdot10^{1}$	ρ_6	—	—	ρ_6	—	—
$h_E^{Z=0.2}(\chi)$	ρ_0	$2.23\cdot10^{3}$	$1\cdot10^{3}$	ρ_0	$8.96\cdot10^{2}$	$5\cdot10^{2}$	ρ_0	$8.49\cdot10^{2}$	$1\cdot10^{3}$
	ρ_1	$-1.70\cdot10^{4}$	$1\cdot10^{4}$	ρ_1	$-7.40\cdot10^{2}$	$6\cdot10^{3}$	ρ_1	$-4.23\cdot10^{3}$	$1\cdot10^{4}$
	ρ_2	$6.85\cdot10^{4}$	$6\cdot10^{4}$	ρ_2	$-5.49\cdot10^{3}$	$3\cdot10^{4}$	ρ_2	$5.12\cdot10^{4}$	$5\cdot10^{4}$
	ρ_3	$-9.64\cdot10^{4}$	$1\cdot10^{5}$	ρ_3	$1.96\cdot10^{4}$	$7\cdot10^{4}$	ρ_3	$-1.72\cdot10^{5}$	$9\cdot10^{4}$
	ρ_4	$2.91\cdot10^{4}$	$1\cdot10^{5}$	ρ_4	$-1.62\cdot10^{4}$	$8\cdot10^{4}$	ρ_4	$2.46\cdot10^{5}$	$1\cdot10^{5}$
	ρ_5	$2.60\cdot10^{4}$	$5\cdot10^{4}$	ρ_5	$9.29\cdot10^{3}$	$4\cdot10^{4}$	ρ_5	$-1.19\cdot10^{5}$	$4\cdot10^{4}$
	ρ_6	$2.31\cdot10^{2}$	$8\cdot10^{1}$	ρ_6	$3.60\cdot10^{2}$	$2\cdot10^{2}$	ρ_6	$4.25\cdot10^{2}$	$2\cdot10^{2}$
$H_E(\chi)$	ρ_0	$-2.12\cdot10^{3}$	$2\cdot10^{3}$	ρ_0	$-3.02\cdot10^{3}$	$1\cdot10^{3}$	ρ_0	$-1.76\cdot10^{3}$	$1\cdot10^{3}$
	ρ_1	$1.40\cdot10^{4}$	$2\cdot10^{4}$	ρ_1	$5.42\cdot10^{3}$	$1\cdot10^{4}$	ρ_1	$4.85\cdot10^{2}$	$1\cdot10^{4}$
	ρ_2	$-7.91\cdot10^{4}$	$9\cdot10^{4}$	ρ_2	$-1.96\cdot10^{3}$	$6\cdot10^{4}$	ρ_2	$2.01\cdot10^{4}$	$5\cdot10^{4}$
	ρ_3	$2.26\cdot10^{5}$	$2\cdot10^{5}$	ρ_3	$-5.51\cdot10^{4}$	$1\cdot10^{5}$	ρ_3	$-1.19\cdot10^{5}$	$1\cdot10^{5}$
	ρ_4	$-3.00\cdot10^{5}$	$2\cdot10^{5}$	ρ_4	$1.20\cdot10^{5}$	$1\cdot10^{5}$	ρ_4	$2.17\cdot10^{5}$	$1\cdot10^{5}$
	ρ_5	$1.51\cdot10^{5}$	$8\cdot10^{4}$	ρ_5	$-6.56\cdot10^{4}$	$7\cdot10^{4}$	ρ_5	$-1.19\cdot10^{5}$	$4\cdot10^{4}$
	ρ_6	$6.28\cdot10^{2}$	$1\cdot10^{2}$	ρ_6	$3.60\cdot10^{2}$	$2\cdot10^{2}$	ρ_6	$4.25\cdot10^{2}$	$2\cdot10^{2}$

		pH = 4.5			pH = 4.75			pH = 5.0	
$h_E^{Z=\infty}(\chi)$	ρ_0	$1.29\cdot10^{3}$	$2\cdot10^{2}$	ρ_0	$4.49\cdot10^{3}$	$2\cdot10^{2}$	ρ_0	$5.33\cdot10^{3}$	$2\cdot10^{3}$
	ρ_1	$2.82\cdot10^{3}$	$1\cdot10^{3}$	ρ_1	$-1.82\cdot10^{4}$	$2\cdot10^{3}$	ρ_1	$-2.97\cdot10^{4}$	$2\cdot10^{4}$
	ρ_2	$6.43\cdot10^{3}$	$5\cdot10^{3}$	ρ_2	$5.78\cdot10^{4}$	$6\cdot10^{3}$	ρ_2	$1.27\cdot10^{5}$	$8\cdot10^{4}$
	ρ_3	$-1.31\cdot10^{4}$	$7\cdot10^{3}$	ρ_3	$-6.51\cdot10^{4}$	$9\cdot10^{3}$	ρ_3	$-2.67\cdot10^{5}$	$2\cdot10^{5}$
	ρ_4	$6.60\cdot10^{3}$	$4\cdot10^{3}$	ρ_4	$2.64\cdot10^{4}$	$4\cdot10^{3}$	ρ_4	$2.95\cdot10^{5}$	$2\cdot10^{5}$
	ρ_5	—	—	ρ_5	—	—	ρ_5	$-1.32\cdot10^{5}$	$8\cdot10^{4}$
	ρ_6	—	—	ρ_6	—	—	ρ_6	$-6.54\cdot10^{2}$	$2\cdot10^{2}$
$h_E^{Z=0.2}(\chi)$	ρ_0	$3.59\cdot10^{3}$	$6\cdot10^{2}$	ρ_0	$9.09\cdot10^{3}$	$2\cdot10^{3}$	ρ_0	$2.51\cdot10^{3}$	$1\cdot10^{3}$
	ρ_1	$-3.81\cdot10^{4}$	$7\cdot10^{3}$	ρ_1	$-9.34\cdot10^{4}$	$2\cdot10^{4}$	ρ_1	$-2.36\cdot10^{4}$	$1\cdot10^{4}$
	ρ_2	$2.09\cdot10^{5}$	$3\cdot10^{4}$	ρ_2	$4.62\cdot10^{5}$	$6\cdot10^{4}$	ρ_2	$1.90\cdot10^{5}$	$5\cdot10^{4}$
	ρ_3	$-5.21\cdot10^{5}$	$8\cdot10^{4}$	ρ_3	$-1.07\cdot10^{6}$	$1\cdot10^{5}$	ρ_3	$-5.81\cdot10^{5}$	$1\cdot10^{5}$
	ρ_4	$6.16\cdot10^{5}$	$8\cdot10^{4}$	ρ_4	$1.17\cdot10^{6}$	$1\cdot10^{5}$	ρ_4	$7.70\cdot10^{5}$	$1\cdot10^{5}$
	ρ_5	$-2.69\cdot10^{5}$	$4\cdot10^{4}$	ρ_5	$-4.78\cdot10^{5}$	$4\cdot10^{4}$	ρ_5	$-3.59\cdot10^{5}$	$4\cdot10^{4}$
	ρ_6	$7.02\cdot10^{2}$	$7\cdot10^{1}$	ρ_6	$8.01\cdot10^{2}$	$1\cdot10^{2}$	ρ_6	$6.45\cdot10^{2}$	$2\cdot10^{2}$
$H_E(\chi)$	ρ_0	$2.30\cdot10^{3}$	$8\cdot10^{2}$	ρ_0	$4.61\cdot10^{3}$	$2\cdot10^{3}$	ρ_0	$-2.82\cdot10^{3}$	$3\cdot10^{3}$
	ρ_1	$-4.09\cdot10^{4}$	$9\cdot10^{3}$	ρ_1	$-7.51\cdot10^{4}$	$2\cdot10^{4}$	ρ_1	$6.19\cdot10^{3}$	$3\cdot10^{4}$
	ρ_2	$2.03\cdot10^{5}$	$4\cdot10^{4}$	ρ_2	$4.05\cdot10^{5}$	$7\cdot10^{4}$	ρ_2	$6.23\cdot10^{4}$	$1\cdot10^{5}$
	ρ_3	$-5.07\cdot10^{5}$	$8\cdot10^{4}$	ρ_3	$-1.00\cdot10^{6}$	$1\cdot10^{5}$	ρ_3	$-3.14\cdot10^{5}$	$3\cdot10^{5}$
	ρ_4	$6.09\cdot10^{5}$	$9\cdot10^{4}$	ρ_4	$1.14\cdot10^{6}$	$1\cdot10^{5}$	ρ_4	$4.75\cdot10^{5}$	$3\cdot10^{5}$
	ρ_5	$-2.69\cdot10^{5}$	$4\cdot10^{4}$	ρ_5	$-4.78\cdot10^{5}$	$4\cdot10^{4}$	ρ_5	$-2.27\cdot10^{5}$	$1\cdot10^{5}$
	ρ_6	$7.02\cdot10^{2}$	$7\cdot10^{1}$	ρ_6	$8.01\cdot10^{2}$	$1\cdot10^{2}$	ρ_6	$1.30\cdot10^{3}$	$4\cdot10^{2}$

2.5 Neutron small-angle scattering (SANS) results

2.5.1 Analysis of SANS patterns from chitosan - $C_{18:1}E_9Ac$ and $C_{18:1}E_9$ complexes

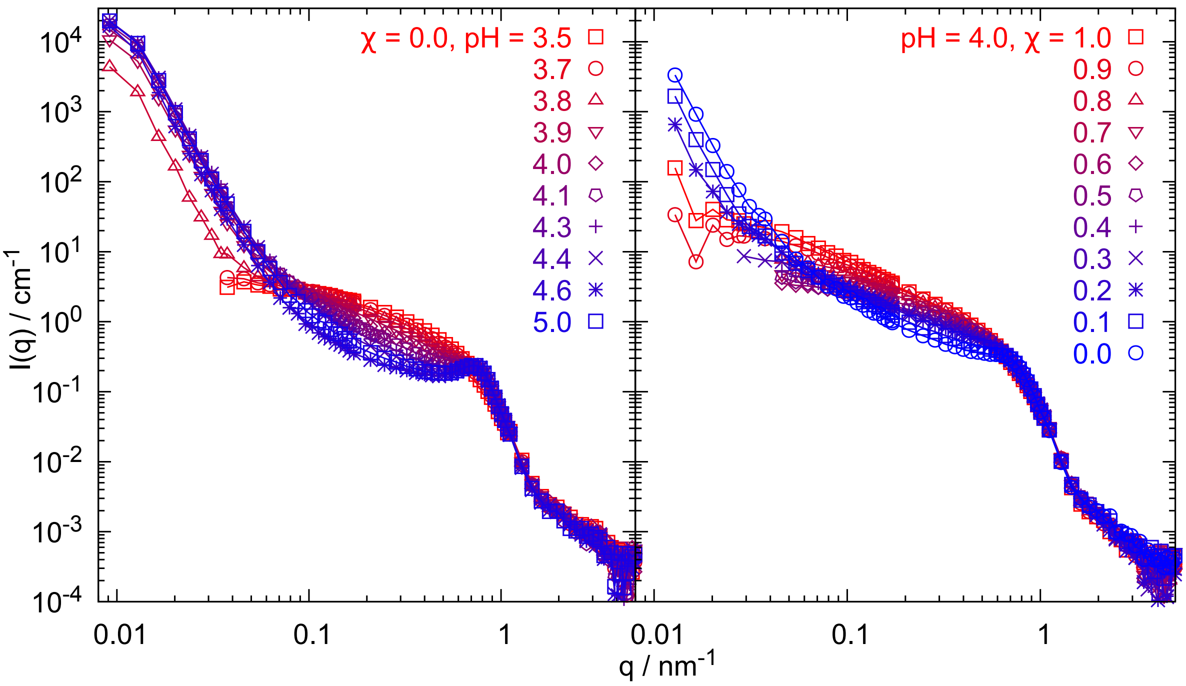

Figure S7: Neutron small-angle scattering (SANS) patterns recorded on V4 at the Helmholtz Zentrum Berlin arising from chitosan chitosan - $C_{18:1}E_9Ac$ and $C_{18:1}E_9$ mixtures, with a chitosan content of 0.3 wt%, $\chi = 0.0$, $Z = 0.2$, and variable pH (on the left) and at pH = 4.0, $Z = 0.2$, and variable χ (on the right). Curves scaled for an improved readability are given in the main text.

SANS patterns arising from chitosan - $C_{18:1}E_9Ac$ and $C_{18:1}E_9$ mixtures are reported in Fig. S9. The data can be quantitatively described using the scattering models described in detail elsewhere.[2] Briefly, three structural models are employed (all analytical expressions are also given in the next section of the supporting information):

(i) when no or only weak interactions between chitosan and the surfactant micelle are present, no evidence for supramolecular aggregation is found. The scattering patterns of a randomly decorated polymer network or independently distributed surfactant micelles and polymer chains in the solution, *i.e.*, no interaction present, are identical. Accordingly, the scattering curves obtained at low pH for $\chi = 0.0$ and at high χ for pH $= 4.0$ were described as a linear superposition of the scattering pattern arising from the chitosan chains, treated as gaussian coils (Eq. S17), and the surfactant micelles, treated as elongated core-shell micelles (Eq. S7).[2,5] The different contributions and the resulting calculated scattering curve are shown in Fig. S8.

(ii) when moderate interactions between chitosan and the surfactant micelle are present. The formation of aggregates with aligned micelles embedded in a chitosan network is found.[2,6] The scattering patterns were described using a model of N aligned core-shell ellipsoids (the micelles) contained in an homogeneous cylinder (the complexed chitosan).[2,7] The scattering form factor is given in Eq. S18. A mass-fractal structure factor with a dimensionality of three is used to take into account the aggregation of the cylindrical subunits (Eq. S23). The model was applied to described the scattering curves from samples with $\chi = 0$ and $3.7 < \text{pH} < 4.3$, and for pH $= 4.0$ and $0.5 < \chi < 1$.

(iii) when strong interactions between chitosan and the surfactant micelle are present the aggregates are found to be collapsed into a core-corona structure, with a core formed by densely packed surfactant micelles surrounded by a stabilizing polymer corona,[2,6] a model initially developed by Berret *et al.*[8] As the size of the micelle and that of the supramolecular aggregate differ by two orders of magnitude (3.5 vs. 150 nm), the scattering form factor can be expressed as the sum of a term arising from dense packed micelles (core-shell ellipsoids with an hard sphere structure factor) and a term from the formed supramolecular structure (a homogeneous core-shell sphere).[2,6] Analytical expressions used for the calculations are given in the next section. The model was applied to described the scattering curves from samples with $\chi = 0$ and pH > 4.05, and for pH $= 4.0$ and $\chi = 1$.

Note that samples found at the border line between the structural picture ii (one-

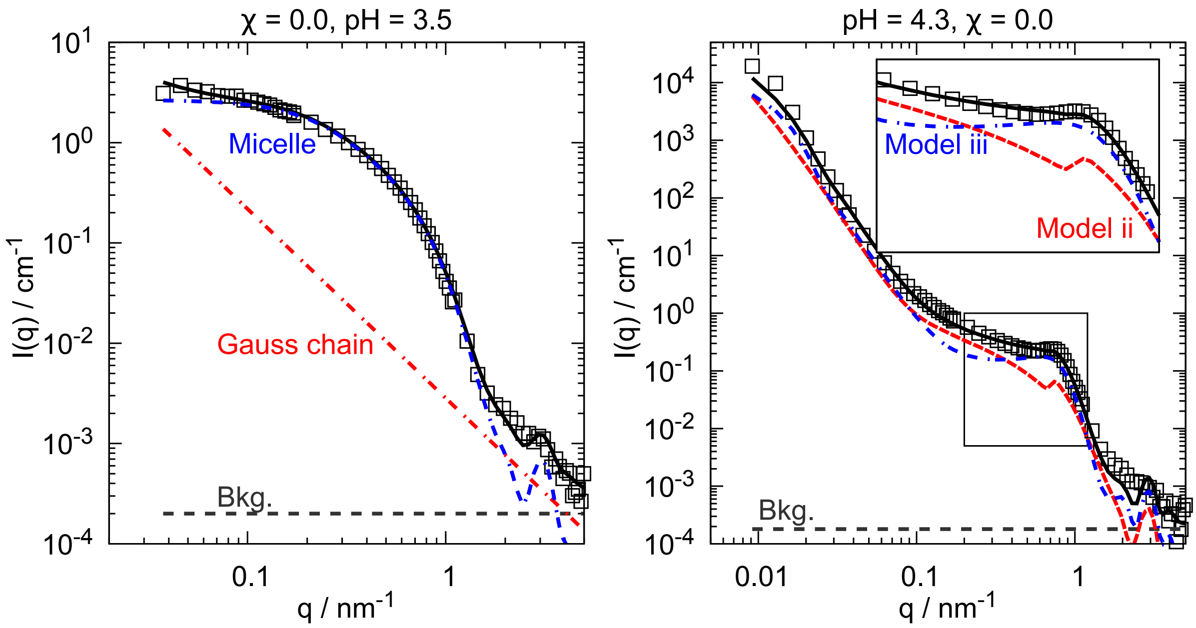

Figure S8: Representative calculations of the SANS patterns. On the left, the scattering curve of a mixture representative for case (i), when no no or weak interaction is present, and the SANS pattern is given by the sum of the contribution of the chitosan gaussian chain (red), the surfactant micelles (blue), and the incoherent background (gray). On the right, the scattering pattern representative for chitosan - surfactant mixtures where the structures described case (ii) and case (iii) coexists. All models are explained in the previous page of the text.

dimensional complex) and iii (core-corona suprastrucure) were described using both models (a representative calculation is given in Fig. S8). Calculated curves and experimental data are reported in Fig. 5 of the main text and in Fig. S9. The parameters used for the calculation of the scattering curves are reported in Table S5.

Table S5: Parameters used for the description of the scattering curves reported in Fig. 5 of the main text and in Fig. S9, determined at different pH and χ values. A, B, and T are the micelle rotational axis, equatorial axis, and shell thickness, respectively and are given in nm; N is the number of micelles per one-dimensional aggregate; ξ is the size of the fractal object whereas r_0 represents the size of the units forming the fractal aggregate and are given in nm; R_{HS} and ϕ_{HS} are the hard sphere radius given in nm and volume fraction of micelles within the dense core of the supramolecular aggregate; R_{core} is the radius of the aggregate and T_{shell} is the thickness of chitosan corona and are given in nm. The values reported in italic were optimized during the fit procedure.

pH	χ	Model	vol% of iii	A	B	T	N	r_0	ξ	R_{HS}	ϕ_{HS}	R_{core}	T_{shell}
3.5	0.0	i	–	*11.3*	*1.9*	*2.0*	–	–	–	–	–	–	–
3.7	0.0	ii	–	*5.5*	*2.0*	*2.0*	*2.1*	*50*	200	–	–	–	–
3.8	0.0	ii	–	*4.0*	*2.0*	*2.0*	*2.8*	*19*	200	–	–	–	–
3.9	0.0	ii	–	*2.9*	*2.0*	*2.0*	*5.0*	*13*	200	–	–	–	–
4.0	0.0	ii + iii	30	*2.6*	*2.0*	*2.0*	*6.5*	*11*	200	*3.6*	*0.18*	130	300
4.1	0.0	ii + iii	50	*2.5*	*2.0*	*2.0*	*7.0*	*10*	200	*3.6*	*0.19*	130	300
4.3	0.0	ii + iii	70	*2.4*	*2.0*	*2.0*	*8.0*	*9*	200	*3.6*	*0.21*	130	300
4.4	0.0	iii	–	*2.4*	*2.0*	*2.0*	–	–	–	*3.5*	*0.20*	130	300
4.6	0.0	iii	–	*2.0*	*2.0*	*2.0*	–	–	–	*3.5*	*0.21*	130	300
5.0	0.0	iii	–	*2.0*	*2.0*	*2.0*	–	–	–	*3.6*	*0.23*	130	300

pH	χ	Model	% of iii	A	B	T	N	r_0	ξ	R_{HS}	ϕ_{HS}	R_{core}	T_{shell}
4.0	1.0	i	–	*100*	*1.9*	*1.7*	–	–	–	–	–	–	–
4.0	0.9	i	–	*50*	*1.9*	*1.7*	–	–	–	–	–	–	–
4.0	0.8	i	–	*28*	*1.9*	*1.7*	–	–	–	–	–	–	–
4.0	0.7	i	–	*13*	*1.9*	*1.7*	–	–	–	–	–	–	–
4.0	0.6	i	–	*10*	*1.9*	*1.7*	–	–	–	–	–	–	–
4.0	0.5	ii	–	*5.0*	*1.9*	*1.9*	*2.1*	–	–	–	–	–	–
4.0	0.4	ii	–	*4.5*	*1.9*	*1.9*	*2.3*	–	–	–	–	–	–
4.0	0.3	ii	–	*4.6*	*1.9*	*1.9*	*5.0*	–	–	–	–	–	–
4.0	0.2	ii	–	*4.3*	*1.9*	*2.0*	*5.5*	*25*	200	–	–	–	–
4.0	0.1	ii	–	*3.8*	*2.0*	*2.0*	*6.0*	*20*	200	–	–	–	–
4.0	0.0	ii + iii	30	*2.6*	*2.0*	*2.0*	*6.5*	*11*	200	*3.6*	*0.18*	130	300

pH	χ	Model	% of iii	A	B	T	N	r_0	ξ	R_{HS}	ϕ_{HS}	R_{core}	T_{shell}
7.0	0.0	iii	–	*2.0*	*2.0*	*2.0*	–	–	–	*3.9*	*0.23*	135	300
7.0	0.15	ii+iii	80	*3.8*	*2.0*	*2.0*	*4.0*	*20*	200	*4.0*	*0.24*	150	300
7.0	0.3	ii+iii	50	*3.5*	*1.9*	*2.3*	*2.5*	*20*	200	*4.5*	*0.23*	150	300
6.0	0.4	ii	–	*3.5*	*2.0*	*1.8*	*6.0*	*20*	200	–	–	–	–
6.0	0.5	ii	–	*6.0*	*2.0*	*2.1*	*2.6*	*28*	200	–	–	–	–
6.0	0.6	ii	–	*7.0*	*2.0*	*2.1*	*2.1*	*35*	200	–	–	–	–
5.0	0.4	ii	–	*4.6*	*2.0*	*1.8*	*6.0*	–	–	–	–	–	–
5.0	0.5	ii	–	*6.0*	*2.0*	*1.8*	*3.0*	*25*	200	–	–	–	–
5.0	0.6	ii	–	*30*	*1.9*	*1.8*	*1.8*	–	–	–	–	–	–

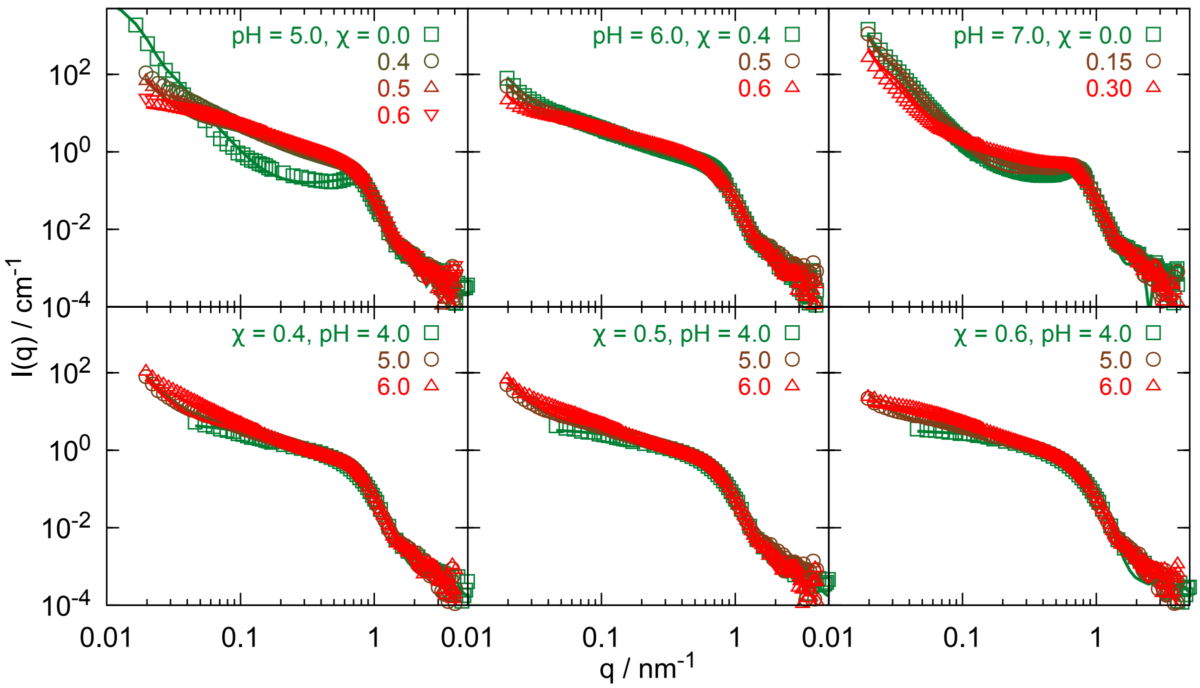

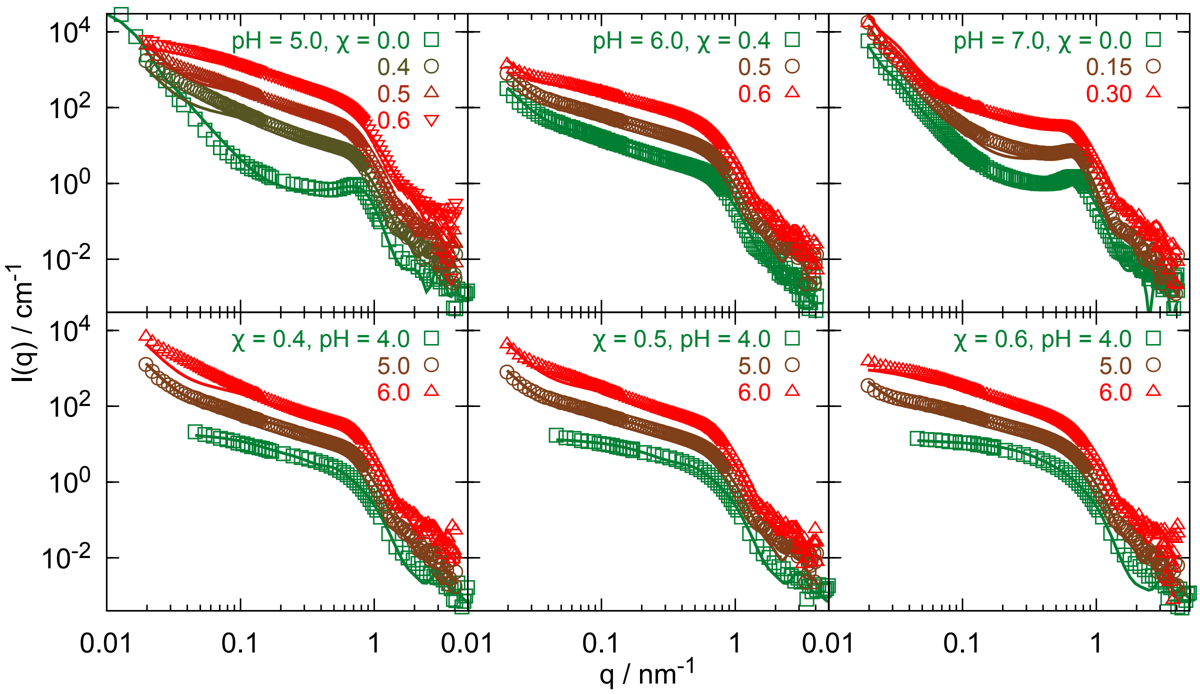

Figure S9: Neutron small-angle scattering (SANS) patterns arising from chitosan - $C_{18:1}E_9Ac$ and $C_{18:1}E_9$ mixtures in the two-phase area, with a chitosan content of 0.3 wt%, $Z = 0.2$, variable pH and variable χ. On the bottom, the same curves are scaled by a factor of three. Full lines are calculated scattering curves with parameters given in Table S5. Data were recorded on D11 at the Institut Laue-Langevin.[9]

2.5.2 Analytical expression for SANS Data analysis

All expression are also reported in the supporting information of Ref. 2 and are reported here for the sake of completeness.

Surfactant Micelle The scattering arising from the surfactant micelles is described using a core-shell ellipsoidal model.[10] The scattering form factor is given by:

$$P_{CS}(q) = \int_0^1 |F(q, \cos\alpha)|^2 \mathrm{d}\cos\alpha \tag{S7}$$

with α being the angle formed by the scattering vector and the rotational axis of the ellipsoid. $F(q, \cos\alpha)$ is the scattering amplitude and is given by

$$F(q, \cos\alpha) = (\mathrm{SLD_c} - \mathrm{SLD_{sh}})\, V_c \left[\frac{3j_1(x_c)}{x_c}\right] + \left(\mathrm{SLD_{sh}} - \overline{\mathrm{SLD}}\right) V_t \left[\frac{3j_1(x_t)}{x_t}\right] \tag{S8}$$

with $\mathrm{SLD_{sh}}$ and $\overline{\mathrm{SLD}}$ being the scattering length densities of the micellar shell and of the medium, respectively. The scattering length density of the shell was obtained as the volume average of the SLDs of the hydrophylic part of the surfactant and the solvent. $j_1(x)$ is the first order spherical Bessel function:

$$j_1(x) = \frac{\sin(x) - x\cos(x)}{x^2} \tag{S9}$$

x_c and x_t are given by:

$$x_c = q\sqrt{A^2\cos\alpha^2 + B^2(1 - \cos\alpha^2)} \tag{S10}$$

$$x_t = q\sqrt{(A+T)^2\cos\alpha^2 + (B+T)^2(1 - \cos\alpha^2)} \tag{S11}$$

and the volumes of the core and of the particle are

$$V_c = \frac{4}{3}\pi AB^2 \tag{S12}$$
$$V_t = \frac{4}{3}\pi(A+T)(B+T)^2 \tag{S13}$$

The particle number density was calculated from the micellar core as

$$^1N = \frac{3\phi_c}{4\pi AB^2} \tag{S14}$$

with phi_c being the volume fraction of the $C_{18:1}$ units. ϕ_c was obtained from the volume fractions of the ionic and nonionic surfactant and the volumes of hydrophilic and hydrophobic part of the surfactant reported in Table S1. The aggregation number from the volume of the hydrophobic tail of the surfactant (v_c)

$$N_{agg} = \frac{4\pi AB^2}{3v_c} \tag{S15}$$

The water content of the shell was calculated as

$$\phi_w^{shell} = \frac{V_{sh} - N_{agg}v_s}{V_{sh}} \tag{S16}$$

with $V_{sh} = V_t - V_c$ being the volume of the hydrated shell and v_s the average volume of the surfactant headgroup.

Chitosan chains The scattering arising from chitosan is described with a gaussian chain model:[11]

$$I(q) = 2 \cdot I(0)_{chi}\frac{e^{-q^2Rg^2} + q^2Rg^2 - 1}{q^4Rg^4} \tag{S17}$$

with $I(0)_{chi}$ and Rg being the forward scattering intensity and the radius of gyration of the polymer chain, respectively. In the calculations, the values of $I(0)_{chi}$ of 20-40 cm^{-1} and $Rg \sim 250$ nm, determined for pure chitosan solutions in Ref. 2 were used.

N aligned core-shell ellipsoids contained in an homogeneous cylinder The scattering form factor for N-aligned globular objects contained in a homogeneous cylinder, as represented in Fig. S10, results from three contributions: the N aligned ellipsoids ($P(q)_{Nob-Nob}$), the cylinder ($P(q)_{Cyl-Cyl}$), and the cross-term ($P(q)_{Nob-Cyl}$):[7]

$$P(q)_{agg} = P(q)_{Nob-Nob} + P(q)_{Cyl-Cyl} + P(q)_{Nob-Cyl} \tag{S18}$$

with

$$P(q)_{Nob-Nob} = \int_0^1 \frac{1-\cos zN_{mic}}{1-\cos z} \Bigg[(\mathrm{SLD_c} - \mathrm{SLD_{sh}})\, V_c \left(\frac{3j_1(x_c)}{x_c}\right) + (\mathrm{SLD_{sh}} - \mathrm{SLD_{cyl}})\, V_t \left(\frac{3j_1(x_t)}{x_t}\right)\Bigg]^2 \mathrm{d}\cos\alpha \tag{S19}$$

$$P(q)_{Cyl-Cyl} = \int_0^1 \left[\left(\mathrm{SLD_{cyl}} - \overline{\mathrm{SLD}}\right) \pi R L^2 j_0\left(\frac{qL\cos\alpha}{2}\right) \frac{J_1(qR\sin\alpha)}{qR\sin\alpha}\right]^2 \mathrm{d}\cos\alpha \tag{S20}$$

$$P(q)_{Nob-Cyl} = \int_0^1 2\frac{\cos\left(\frac{z\,N_{mic}}{2}\right)\,\sin\left(\frac{z\,N_{mic}+z}{2}\right) - \sin\left(\frac{z}{2}\right)}{\sin\left(\frac{z}{2}\right)} \Bigg[(\mathrm{SLD_c} - \mathrm{SLD_{sh}})\, V_c \left(\frac{3j_1(x_c)}{x_c}\right) + (\mathrm{SLD_{sh}} - \mathrm{SLD_{cyl}})\, V_t \left(\frac{3j_1(x_t)}{x_t}\right)\Bigg] \cdot \left[\left(\mathrm{SLD_{cyl}} - \overline{\mathrm{SLD}}\right)^2 \pi R L^2 j_0\left(\frac{qL\cos\alpha}{2}\right) \frac{J_1(qR\sin\alpha)}{qR\sin\alpha}\right] \mathrm{d}\cos\alpha \tag{S21}$$

with $z = qD\cos\alpha$, $j_0(x) = \sin(x)/x$ and $J_1(x)$ the first-order cylindrical Bessel function of the first kind. x_c and x_t are defined in Eqs. S10 and S11. N_{mic} is the number of ellipsoids

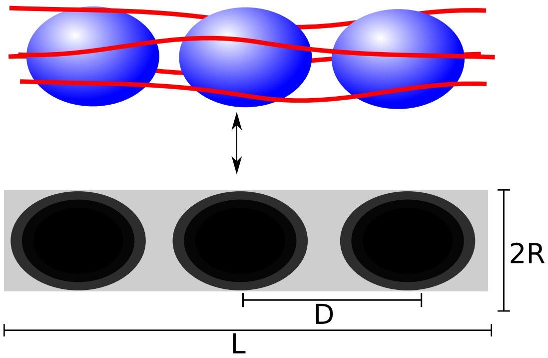

Figure S10: Schematic representation of the structure formed by stiff polyelectrolytes and weakly charged macroions. Such a structure can be approximated with a particles in a cylinder model, characterized by an overall extension L, a radius R and a spacing between the centers of the objects of D.

per cylinder and D the spacing between their centers. The scattering length densities were calculated assuming an anhydrous micellar core, a micellar core composed of water and the hydrophilic part of the surfactant, and the cylinder being made of chitosan and solvent. The amount of chitosan in the cylinder is calculated in such a way that charge neutrality is reached within the cylinder. The number density of the cylinders is obtained assuming all surfactant being involved in the complex:

$$ {}^{1}N_{cyl} = \frac{{}^{1}N}{N_{mic}} = \frac{3\phi_c}{4\pi N_{mic} AB^2} \tag{S22}$$

A mass-fractal structure factor is used to describe the supramolecular aggregation of the cylindrical building blocks:[2]

$$ S(q)_{agg} = 1 + \frac{3\sin\left(3\arctan(q\xi)\right)}{(qr_0)^3\left[1+\frac{1}{q^2\xi^2}\right]} \tag{S23}$$

Densely packed micelles in a supramolecular core-shell structure The scattering pattern arising from a supramolecular core-shell structure formed by a core of densely packed micelles glued together by chitosan and stabilized by a chitosan shell was obtained as:[2]

$$I(q) = {}^1N_{SA}P_{SA}(q) + {}^1NP_{CS}(q)S_{HS}(q) \tag{S24}$$

with $P_{SA}(q)$ being the scattering form factor of a homogeneous core-shell sphere, $S_{HS}(q)$ is the hard-sphere structure factor:[12]

$$S_{HS}(q) = \left(1 - {}^1NC_0(q)\right)^{-1} \tag{S25}$$

with

$$\begin{aligned} {}^1NC_0(q) \quad = \quad & \frac{\Lambda}{x^3}(\sin x - x\cos x) + \frac{\Upsilon}{x^3}\left(\left(\frac{2}{x^2} - 1\right)x\cos x + 2\sin x - \frac{2}{x}\right) \\ & -\frac{\Lambda\phi_{HS}}{2x^3}\left[\frac{24}{x^3} + 4\left(1 - \frac{6}{x^2}\right)\sin x - \left(1 - \frac{12}{x^2} + \frac{24}{x^4}\right)x\cos x\right] \end{aligned} \tag{S26}$$

with $x = 2R_Sq$, $\Lambda = -24\phi_{HS}\left(\frac{1+2\phi_{HS}}{(1-\phi_{HS})^2}\right)^2$ and $\Upsilon = 36\left(\phi_{HS}\frac{2+\phi_{HS}}{(1-\phi_{HS})^2}\right)^2$.

Given the large difference in size between the surfactant micelle and the supramolecular aggregate, the micelle-aggregate cross-term was neglected. The scattering form factor of the supramolecular aggregate is obtained as:

$$\begin{aligned} P_{SA}(q) = \Bigg[& V_c^{SA}\left(\mathrm{SLD}_{\mathrm{c}}^{SA} - \mathrm{SLD}_{\mathrm{sh}}^{SA}\right)\frac{3\sin\omega_c - 3\omega_c\cos\omega_c}{{\omega_c}^3} + \\ & V_t^{SA}\left(\mathrm{SLD}_{\mathrm{sh}}^{SA} - \overline{\mathrm{SLD}}\right)\frac{3\sin\omega_{sh} - 3\omega_{sh}\cos\omega_{sh}}{\omega_{sh}^3}\Bigg]^2 \end{aligned} \tag{S27}$$

with $\mathrm{SLD}_{\mathrm{c}}^{SA}$, $\mathrm{SLD}_{\mathrm{sh}}^{SA}$, V_c^{SA} and V_t^{SA} being the scattering length densities of the core and the shell of the supraaggregate, and the volume of the core and the total volume of the SA, respectively. $\omega_c = qR_c^{SA}$ and $\omega_{sh} = qR_{sh}^{SA}$ with R_c^{SA} and R_s^{SA} being the radii of the core and the shell of the supraaggregate, respectively. For the calculation a normal distribution of R_c^{SA} with a relative standard deviation 0.3 was assumed.

The number of micelles in the supraaggregate core was obtained combining the radius of the supraaggregate and the hard-sphere radius and volume fraction:

$$N_{mic} = \frac{\left\langle R_c^{SA^3} \right\rangle}{R_{HS}^3} \phi_{HS} \tag{S28}$$

Accordingly, the supraaggregate number density is given by:

$$^1N_{SA} = \frac{^1N}{N_{mic}} = \frac{3\phi_c}{4\pi N_{mic} AB^2} \tag{S29}$$

The scattering length density of the core of the supraaggregate was calculated as the volume weighted average of the components (surfactants, chitosan, and solvent):

$$\mathrm{SLD}_{\mathrm{c}}^{SA} = \frac{N_{mic} N_{agg} \left(v_c + v_s\right)}{4/3\pi R_c^{SA^3}} \mathrm{SLD}_{\mathrm{surf}} + \frac{\phi_{ch} \chi_{core}^{chi} v_{ch}}{4/3\pi R_c^{SA^3}} \mathrm{SLD}_{chi} + \frac{\left(4/3\pi R_c^{SA^3} - N_{mic} N_{agg} \left(v_c + v_s\right) - \phi_{ch} \chi_{core}^{chi} v_{ch}\right)}{4/3\pi R_c^{SA^3}} \mathrm{SLD}_{\mathrm{solv}} \tag{S30}$$

and the scattering length density of the shell of the supraaggregate as

$$\mathrm{SLD}_{\mathrm{sh}}^{SA} = \frac{\phi_{ch} \chi_{sh}^{chi} v_{ch}}{4/3\pi R_s^{SA^3} - 4/3\pi R_c^{SA^3}} \mathrm{SLD}_{chi} + \frac{\left(4/3\pi R_s^{SA^3} - 4/3\pi R_c^{SA^3} - \phi_{ch} \chi_{sh}^{chi} v_{ch}\right)}{4/3\pi R_s^{SA^3} - 4/3\pi R_c^{SA^3}} \mathrm{SLD}_{\mathrm{solv}} \tag{S31}$$

2.6 Characterization of pure surfactant mixtures

The mixing behavior of the ionic $C_{18:1}E_9CH_2COOH$ and the nonionic $C_{18:1}E_9$ was investigated both from a thermodynamic and structural perspective. The excess mixing enthalpy were determined *via* calorimetric titrations (Eqs. 3 and 4 of the main text) and are reported in Fig. S11. Given the chemical similarity of the surfactant, we made use of the regular solution theory for the description of the thermodynamics of the mixing

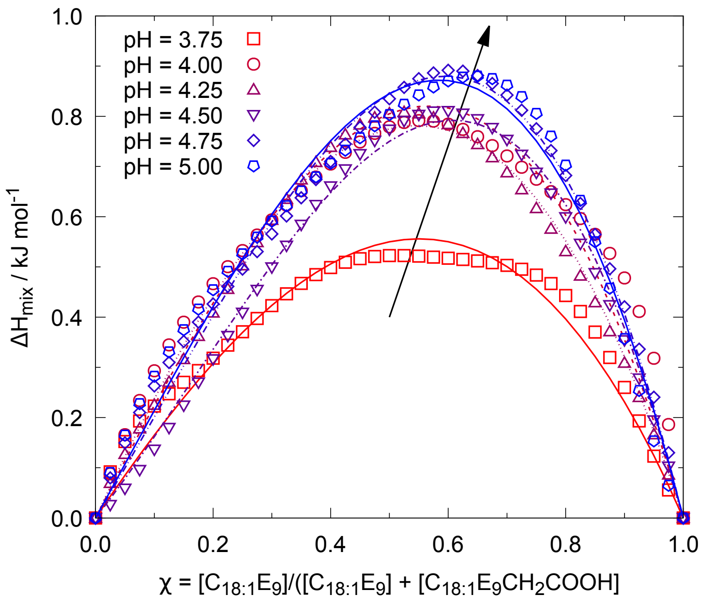

Figure S11: Mixing enthalpies determined at a total surfactant concentration of $\sim 10^{-3} mol L^{-1}$ and at variable pH, as a function of non-ionic surfactant content χ. Full lines are fits according to Eq. S34. Arrow indicates effect of increasing pH.

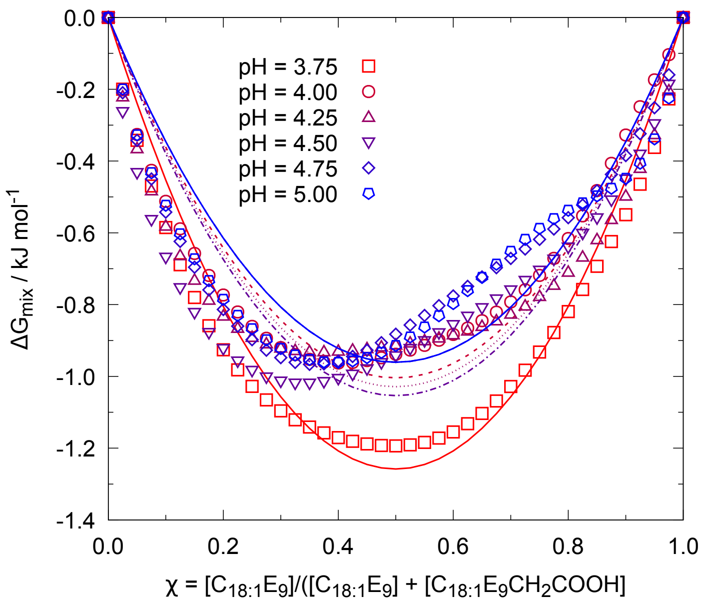

Figure S12: Gibbs free energy of mixing determined at a total surfactant concentration of $\sim 10^{-3} mol L^{-1}$ and at variable pH, as a function of non-ionic surfactant content χ.

process. Accordingly, the molar mixing entropy for ideal mixing is given by:[13]

$$T\overline{\Delta \mathrm{S}}_m = -RT\left[\chi \ln \chi + (1-\chi)\ln(1-\chi)\right] \tag{S32}$$

with R being the ideal gas constant and T the absolute temperature. The combination of experimentally determined mixing enthalpy (Fig. S11) and calculated mixing entropy leads to the mixing free energy (Fig. S12). The mixing enthalpy can be expressed as a polynomial expansion:

$$\overline{\Delta \mathrm{H}}_m = \chi(1-\chi)\sum_{i=1} A_i(2\chi-1)^{i-1} \tag{S33}$$

Developing the series only to its first term leads to the simple expression $\overline{\Delta \mathrm{H}}_m = A\chi(1-\chi)$, also known as the Porter equation.[14] Given the slight asymetric shape of the excess mixing enthalpy curves, with the maximum around 0.6, Eq. S33 was developed up to the second term, leading to

$$\overline{\Delta \mathrm{H}}_m = \chi(1-\chi)\left[A + B(2\chi-1)\right] \tag{S34}$$

The free energy of mixing was described as:[15]

$$\overline{\Delta \mathrm{G}}_m/RT = \beta\chi(1-\chi) \tag{S35}$$

The mixing enthalpy and the free energy of mixing were fitted with Eqs. S34 and S35, respectively. The obtained values are reported in Table S6. All mixing processes are slightly endothermic, as also found in several surfactant/lipid mixtures.[16] However, the enthalpic contribution is compensated by the mixing entropy, resulting in an exergonic process, i.e. fully miscible micelles are formed, as expected from the chemical similarity of both headgroup and tail (see Fig. S12). Although the simple, first order development

Table S6: Parameters used for the description of the mixing enthalpy and mixing free energy of the ionic $C_{18:1}E_9CH_2COOH$ and the nonionic $C_{18:1}E_9$ surfactant.

pH	A / J mol^{-1}	B / J mol^{-1}	β
3.75	2200 ± 30	460 ± 70	-2.03 ± 0.03
4.00	3220 ± 50	900 ± 100	-1.62 ± 0.03
4.25	3100 ± 20	1500 ± 40	-1.66 ± 0.04
4.50	3000 ± 20	1500 ± 50	-1.70 ± 0.05
4.75	3400 ± 20	1400 ± 60	-1.55 ± 0.04
5.00	3400 ± 60	1250 ± 100	-1.55 ± 0.04

of the free energy reported in Eq. S35 does not capture the whole complexity of the system, it offers a useful approach for comparing the β parameter with values found in similar systems. In fact, the values for this system of $-2 < \beta < -1.5$ fall within the usual range of anionic-nonionic ethoxylated surfactant mixtures.[15] With increasing pH, i.e. with increasing charge density of the ionic species, the process becomes more endothermic and more asymmetric, as evidenced also by the increasing values of A and B of Eq. S34. This observation can be explained by the fact that with increasing degree of ionization of the surfactants, a larger difference between the headgroups is observed: the area per molecule at the core-shell interface of the surfactant micelle for $C_{18:1}E_9CH_2COOH$ increases from 59 to 69 Å^2 when pH is varied between 2.7 and 6.2.[5] As a comparison, the headgroup area of $C_{16}E_9$ at the air-water interface is 53 Å^2.[17]

The headgroup size difference is also clearly visible in the micelle aggregation numbers and hydrodynamic radii, as determined by static and dynamic light scattering, respectively (see Fig. S13). With increasing nonionic surfactant content the micelles grow in size, with an hydrodynamic radius increasing from ca. 5 to almost 25 nm, and the aggregation number increasing from ca. 200 to above 3000 molecules per micelle. This is a consequence of an effective decrease of headgroup area requirement, resulting in a larger packing parameter. Almost no differences are observed between mixtures at pH 4.5 and 5.0, while the growth process takes place at lower χ for the more weakly charged system at pH 4.0. The results are in good agreement with previous SANS experiments performed on $C_{18:1}E_9CH_2COOH$ between pH 2.5 and 10, showing a transition from rodlike to globular micelles upon acidification.[5]

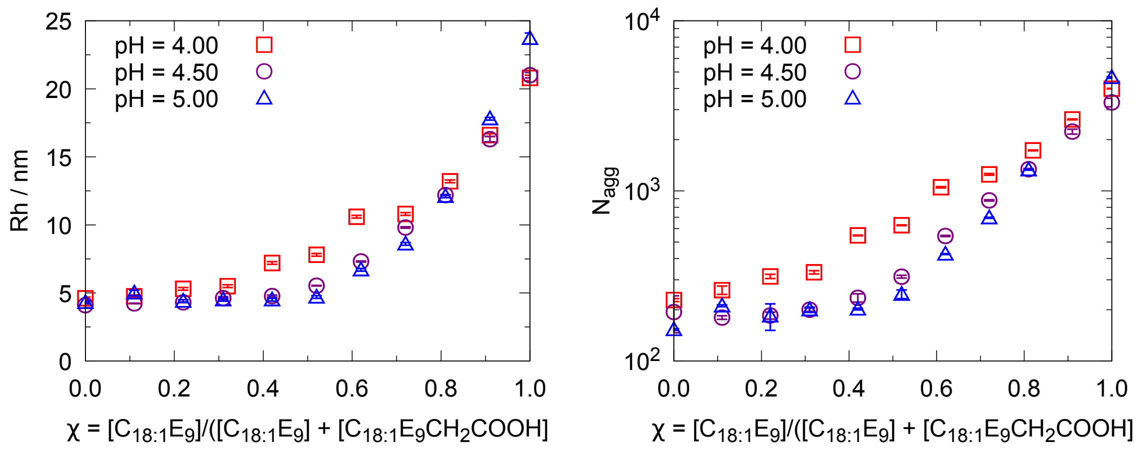

Figure S13: Hydrodynamic radius (left) and aggregation number (right) determined *via* light scattering experiments at a total surfactant concentration of 1 wt% and at variable pH, as a function of non-ionic surfactant content χ.

To probe the ionization condition of the micellar aggregate ζ-potential experiments were carried out and are reported in Fig. S14. The different pH has no effect on the determined ζ-potential values, as the additional charges arising from the increased degree of ionization of $C_{18:1}E_9CH_2COOH$ are compensated by condensed counterions. Moreover, two regions can be identified in the evolution of the ζ-potential with χ: below $\chi = 0.4$, where a ζ-potential value of ca. -25 mV is determined; and for $\chi > 0.4$, where the potential approaches zero, till a neutral surface is obtained for $\chi = 1$, i.e., the pure nonionic surfactant. Similar values are found in other ionic/nonionic mixed micellar systems determined at salt content ~ 0.2 M, as it was in our case.[18,19]

2.7 Ionization degree of pure components

In Fig. S15 the degree of ionization of chitosan and $C_{18:1}E_9CH_2COOH$ as a function of pH is reported. Titration were performed adding a 0.1 mol L^{-1} standard NaOH solution to a 1 wt% solution of chitosan or $C_{18:1}E_9CH_2COOH$ in the presence of 1 mol L^{-1} HCl.

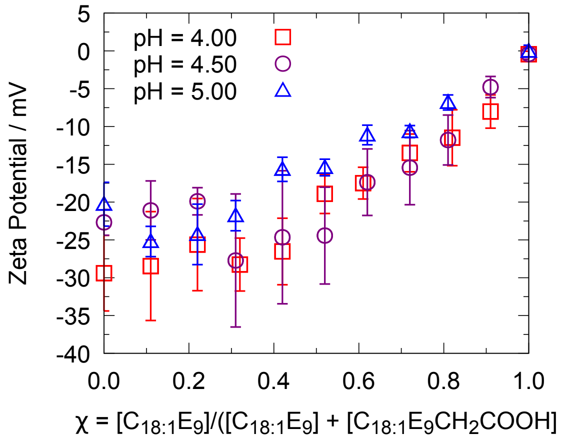

Figure S14: ζ-potential determined at a total surfactant concentration of 1 wt% and at different pH, as a function of non-ionic surfactant content χ.

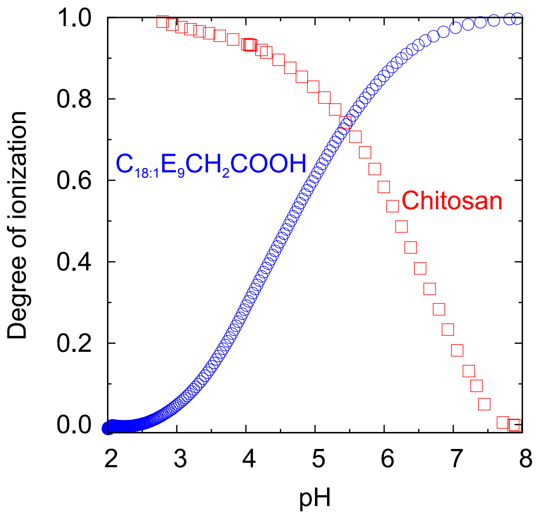

Figure S15: Degree of ionization of Chitosan and $C_{18:1}E_9CH_2COOH$ in H_2O as a function of pH obtained from potentiometric titration.

References

(1) Itakura, M.; Shimada, K.; Matsuyama, S.; Saito, T.; Kinugasa, S. A convenient method to determine the Rayleigh ratio with uniform polystyrene oligomers. *J. Appl. Polym. Sci.* **2006**, *99*, 1953–1959.

(2) Chiappisi, L.; Prévost, S.; Grillo, I.; Gradzielski, M. Chitosan/alkylethoxy carboxylates: A surprising variety of structures. *Langmuir* **2014**, *30*, 1778–1787.

(3) Frisken, B. J. Revisiting the Method of Cumulants for the Analysis of Dynamic Light-Scattering Data. *Appl. Opt.* **2001**, *40*, 4087.

(4) Swan, J. W.; Furst, E. M. A simpler expression for Henry's function describing the electrophoretic mobility of spherical colloids. *J. Colloid Interface Sci.* **2012**, *388*, 92–94.

(5) Schwarze, M.; Chiappisi, L.; Prévost, S.; Gradzielski, M. Oleylethoxycarboxylate An efficient surfactant for copper extraction and surfactant recycling via micellar enhanced ultrafiltration. *J. Colloid Interface Sci.* **2014**, *421*, 184–190.

(6) Chiappisi, L.; Prévost, S.; Grillo, I.; Gradzielski, M. From Crab Shells to Smart Systems: ChitosanAlkylethoxy Carboxylate Complexes. *Langmuir* **2014**, *30*, 10608–10616.

(7) Chiappisi, L.; Prévost, S.; Gradzielski, M. Form factor of cylindrical superstructures composed of globular particles. *J. Appl. Crystallogr.* **2014**, *47*, 827–834.

(8) Berret, J.-F.; Hervé, P.; Aguerre-Chariol, O.; Oberdisse, J. Colloidal Complexes Obtained from Charged Block Copolymers and Surfactants: A Comparison between Small-Angle Neutron Scattering, Cryo-TEM, and Simulations. *J. Phys. Chem. B* **2003**, *107*, 8111–8118.

(9) Gradzielski, M.; Chiappisi, L.; Hoffmann, I.; Schweins, R.; Simon, M.; Yalcinkaya, H. Interconnecting charged microemulsion droplets via oppositely charged polyelectrolyte - effect of polyelectrolyte structure. 2016.

(10) Bendedouch, D.; Chen, S. H. Effect of an attractive potential on the interparticle structure of ionic micelles at high salt concentration. *J. Phys. Chem.* **1984**, *88*, 648–652.

(11) Debye, P. Molecular-weight Determination by Light Scattering. *J. Phys. Colloid Chem.* **1947**, *51*, 18–32.

(12) Baba-Ahmed, L.; Benmouna, M.; Grimson, M. J. Elastic Scattering from Charged Colloidal Dispersions. *Phys. Chem. Liq.* **1987**, *16*, 235–238.

(13) Hoffmann, H.; Poessnecker, G.; Possnecker, G. The Mixing Behavior of Surfactants. *Langmuir* **1994**, *10*, 381–389.

(14) Porter, A. W. On the vapour-pressures of mixtures. *Trans. Faraday Soc.* **1920**, *16*, 336.

(15) Rosen, M. J. *Surfactants and interfacial phenomena surfactants and interfacial phenomena*, 3rd ed.; John Wiley & Sons, Inc.: Hoboken, New Jersey., 2004; p 455.

(16) Heerklotz, H.; Seelig, J. Titration calorimetry of surfactantmembrane partitioning and membrane solubilization. *Biochim. Biophys. Acta - Biomembr.* **2000**, *1508*, 69–85.

(17) Elworthy, P. H.; Macfarlane, C. B. Surface activity of a series of synthetic non-ionic detergents. *J. Pharm. Pharmacol.* **1962**, *14*, 100T–102T.

(18) Tokiwa, F. Solubilization behavior of mixed surfactant micelles in connection with their zeta potentials. *J. Colloid Interface Sci.* **1968**, *28*, 145–148.

(19) Micheau, C.; Schneider, A.; Girard, L.; Bauduin, P. Evaluation of ion separation coefficients by foam flotation using a carboxylate surfactant. *Colloids Surfaces A Physicochem. Eng. Asp.* **2015**, *470*, 52–59.